

## RANDOM FIELD OF THE MODULUS OF ELASTICITY CONSIDERING KNOTS: APPLICATION TO WOOD UTILITY POLES

Laura V. González de Paz<sup>a,d</sup>, Diego A. García<sup>b,c</sup>, Néstor F. Ortega<sup>a,d</sup> and Marta B. Rosales<sup>a,e</sup>

<sup>a</sup>*Department of Engineering, Universidad Nacional del Sur, Bahía Blanca, Argentina,  
dtoinge@uns.edu.ar, <http://www.uns.edu.ar/deptos/ingenieria>.*

<sup>b</sup>*CONICET, Argentina.*

<sup>c</sup>*Department of Civil Engineering, Universidad Nacional de Misiones, Oberá, Argentina.*

<sup>d</sup>*Instituto de Ingeniería - Universidad Nacional del Sur - CIC, Buenos Aires, Argentina.*

<sup>e</sup>*IFISUR – Universidad Nacional del Sur - CONICET, Bahía Blanca, Argentina.*

**Keywords:** Wood Pole, Uncertain Material Properties, FEM, Experimental Mechanics.

**Abstract.** Wood utility poles are simple structures used in power networks and their failure can produce a significant impact on their reliability as well as economic consequences. The presence of knots is known to be the main source of the lengthwise variability and reduction in bending strength and stiffness in wood elements. Other authors have studied this variability and developed Modulus of Elasticity (MOE) distribution models for sawed wood elements, like beams. The aim of this work is to determine whether the aforementioned models, originally developed for sawn wood beams, can be applied to a wood structure without sawing such as wood utility poles. Load-displacement curves and natural frequencies of the poles were obtained from static and dynamic test, respectively. A visual survey was also carried out to record geometry data, knot dimensions and location in the poles. Numerical models considering the surveyed geometry and the presence of knots are used. With this approach, the MOE random field is simulated through a weak zone model that accounts for knots. The governing equations are discretized through the Finite Element Method (FEM). The stochastic analysis is performed by means of Monte Carlo Simulations (MCS). Then, experimental data (displacements and natural frequencies) are compared with numerical results in order to determine whether the models developed for sawn beams can be applied to wood utility poles.

## 1 INTRODUCTION

Utility poles made of timber are widely used in all the world because they are of relative low cost and environmentally friendly. *Eucalytus grandis* is extensively used in Argentina for structural purposes, in particular, utility poles. Some standards indicate the procedures to determine the mechanical properties of wood ( [ASTM D 143-94, 2007](#); [ASTM D 198, 2002](#)) and particularly of wood poles ( [ASTM D 1036, 2005](#)). Studies of the mechanical properties of this particular species were made by [Piter \(2003\)](#); [Piter et al. \(2004\)](#), and particularly in utility poles by [Torrán et al. \(2009\)](#).

Due to its natural origin, structural timber is characterized by considerable lengthwise variability in its mechanics properties. However these properties are treated as random variables and their spatial variability is not taken into account in design practice. Growth defects such as knots, often related to localized grain deviation, are the main source of the lengthwise variability of bending strength and stiffness in a timber piece. The presence of grain deviation can decrease the modulus of elasticity (MOE) in the longitudinal direction. Knots are unavoidable in structural timber, the effective MOE in the longitudinal direction varies along the axis of a wood structural piece, even more in pieces of wood without sawing. In [García et al. \(2015\)](#); [García and Rosales \(2017\)](#) some models that describe the variation of mechanical properties due to the presence of defects were proposed for beam elements.

Due to the variability in their mechanical properties, in particular the lengthwise variability of MOE, a stochastic approach is necessary in order to attain a more realistic structural model. Therefore, a realistic response of structural components subjected to external demands is desirable.

The authors studied the response of wooden poles simulating the longitudinal variation of the MOE with random fields, with different approaches ([Gonzalez de Paz et al., 2016, 2017](#)), based on the values of global MOE published in [Piter et al. \(2004\)](#) for poles of *Eucalyptus grandis*, and local MOE as a function of knot ratio in a given section, obtained for sawn wood.

The main aim of this work is to verify if the parameters found for sawn wood are valid for wood without sawing. To do this, field models describing the variation of the MOE were made using the survey of position and size of knots on real poles ([Gonzalez de Paz et al., 2018](#)). Then, the calculated fields were applied to structural models and the results were compared with the records of the tests of those surveyed poles, studying the response in displacement and in frequency.

## 2 EXPERIMENTAL DETERMINATIONS

As a first step, measurements of geometry, and size and position of knots on a sample of real poles were made. Then, natural frequencies measurements and load-displacement test were carried out. The test sample consisted of six impregnated real-sized poles which different degrees of deterioration after a period of service. They were provided by the electricity company, Empresa Distribuidora de Energía del Sur (EDES). Different tests were carried out on this sample, to determine: modulus of elasticity, density, natural frequencies.

### 2.1 Survey of geometry and knots

A survey of geometrical dimensions was carried out. The actual length and circumference at base, tip, ground line, the loading point, at every 0.60 m from the base, and every 0.50 m were measured and recorded for each pole. Although the poles had different total lengths, it should be noted that after the clamping, the free length resulted in 5 m for all the poles. Table 1 depicts

the main geometry data of the 6 poles.

Pole	Circunference at		Length (m)
	ground line at 5 m from tip (mm)	tip (mm)	
1	435	347	6.3
2	510	452	5.9
3	445	352	6.5
4	515	447	6.0
5	540	475	6.1
6	547	449	7.5

Table 1: Main geometry data of the poles.

In accordance with the criterion adopted by the American standard [ANSI-05.1 \(2002\)](#), the dimension of a knot was considered equal to its diameter on the surface of the pole in a direction perpendicular to the length axis. Its position was measured parallel and perpendicularly from a reference line of same direction that the length axis. Dimension and location of all knots were taken and recorded. The measurements, for both geometry and knots, were later used to assemble the numerical models.

## 2.2 Natural frequencies measurements

On the other hand, prior to carrying out the load-displacement test, the first three natural frequencies were measured experimentally. For the experimental determination of the frequencies, a modal impact test was performed, by hitting the pole with a rubber hammer and recording the accelerations with accelerometer sensors placed on the tip of each pole. The frequencies were obtained through a Fast Fourier Transform (FFT) of the the acceleration-time signal records. The results obtained are illustrated in columns 4 to 6 of the Table 2.

## 2.3 Load-displacement test

After physical measurements were taken and recorded, cantilever bending tests were carried out according to the procedures of the American standard [ASTM D 1036 \(2005\)](#) which were also adopted by the Argentinean standard [IRAM 9529 \(2005\)](#). Each pole was placed in the testing setup so that its ground line coincided with the front face of the crib. The ground line distance from base was at least 15% the length of the shortest pole and at 5 m from the tip. The loading point was located at 0.6 m from the tip in all cases. From the measurements, for each pole, the modulus of elasticity  $MOE_{Standard}$  was determined, as indicated by the aforementioned standards ([ASTM D 1036, 2005](#)). The results are shown in column 1 of the Table 2.

## 2.4 Density test

The density values were determined according to the procedures established in [ISO 3131:1975 \(1975\)](#), using a knot-free disk taken from the proximity of the fixing point after the static test. The density values obtained were used in the subsequent numerical models. The results of the mean density value  $\rho$  are shown in the third column of Table 2.

## 2.5 Summary of experimental tests

The results of the above-mentioned tests (MOE, density, natural frequencies) are summarized in Table 2.

Pole	MOE <sub>Standard</sub> (MPa)	$\rho$ (kg/m <sup>3</sup> )	1 <sup>st</sup> freq (Hz)	2 <sup>nd</sup> freq (Hz)	3 <sup>rd</sup> freq (Hz)
1	10004	580	3.60	19.53	50.96
2	11902	653	3.61	20.36	54.25
3	11907	580	3.80	20.21	53.80
4	10315	550	4.05	22.50	59.27
5	9314	578	4.05	22.70	62.93
6	14597	750	4.39	23.14	60.50

MOE<sub>Standard</sub>: Modulus of Elasticity according to [ASTM D 1036 \(2005\)](#);  
 $\rho$ : average value of the density.

Table 2: Summary of the results of the tests carried out on the poles.

## 3 NUMERICAL SIMULATIONS

Numerical simulations were carried out to determine the lengthwise variability of the Modulus of Elasticity (MOE). To do this, the weak zones model was used, based on the surveyed data of geometry and knots of the poles, and the marginal distributions as a function of the knot ratio  $K$ . Then the structural models were constructed to calculate displacements as function of load, and natural frequencies. These results were compared with those recorded in the tests in the previous section.

### 3.1 MOE as random field with the Weak Zone model

For the construction of the model that describes the MOE, Weak Zone modeling consists in the following steps:

- Determine the clear wood sections and the sections with knots, taking into account that the length of the weak zones are proportional to five times the knot dimension. When the influence lengths between knots overlap, it is considered as a group belonging to the same section.
- For each section with knots, calculate the knot ratio and compare with the reference knot ratio. According to the relationship between these, the corresponding parameters are assigned for the MOE values calculation. Spatial correlation of MOE values is considered by Nataf transformation with gamma marginal PDF in each section.

#### 3.1.1 Lengthwise variability of the MOE

Structural timber is composed of both wood with and without defects. The knots affect the mechanical properties considerably. The MOE along the pole is modeled as a composite of weak zones connected by sections of clear wood. Weak zones correspond to knots or groups of knots.

Weak zones were determined from a visual survey of knots for each pole, considering a length of influence of each knot equal to five times its dimension parallel to longitudinal pole

axis. If sections of influence between two knots overlapped, both were considered to belong to the same section.

The knot ratio  $k_1$  of each section was calculated as the relation between the transversal dimension of the knot and the average circumference of the affected section. In case the section contained more than one node, the relationship between the sum of the nodes and the average circumference was considered. Then, the  $k_1$  values were compared with a reference value  $k_{ref}$  proposed by the standard [CIRSOC 601 \(2011\)](#), which takes the relationship between the maximum diameter allowed for a knot and the circumference of the pole section in which it is located.

Knot ratio  $K = \frac{k_1}{k_{ref}}$  values were classified and the values of the parameters of the marginal PDF according to [Table 3](#) were assigned to each section.

### 3.1.2 Nataf transformation and marginal PDF

Nataf transformation is employed in order to generate and simulate the random field. Introduced by [Der Kiureghian and Liu \(1986\)](#), it allows to build a multidimensional PDF that fit a prescribed marginal distribution and a correlation matrix. The procedure used is described in the work of [García et al. \(2015\)](#).

The parameters of the marginal PDF of MOE were found experimentally by [Piter \(2003\)](#) and classified by [García \(2017\)](#) according to  $K$  knot ratio. These values are depicted in [Table 3](#):

Parameters	$K = 0$	$0 \leq K \leq 1/3$	$1/3 \leq K \leq 2/3$	$2/3 \leq K$
$\mu$ (Gpa)	15.89	13.46	12.87	11.63
$\sigma$ (Gpa)	2.83	2.06	2.16	1.95

Table 3: Parameters for the gamma marginal PDF of the MOE for each  $K$  value.

## 3.2 Structural model

The numerical model consisted of a Euler beam clamped at the ground line and subjected to a load at 0.6 m from the free tip, with the geometry according to the recorded data (main measures depicted in [Table 1](#)) and taking into account the surveyed knots. The density values were determined by the standard [ISO 3131:1975 \(1975\)](#) and the MOE assigned to each pole corresponds to the one determined in the previous section.

The load at the tip was taken equal to that registered at each point of displacement in the experimental test, in order to emulate the displacements at the point of application of the load and compare with the measured results.

A numerical modal analysis was carried out in order to obtain the natural frequencies, which were then compared with the outcomes of the corresponding test. The software used was [Flex-PDE, PDE \(2017\)](#) based in a finite elements discretization, with 50 quadratic type elements, and the results were processed with the Matlab software. A Monte Carlo method is used to perform the realizations within the Matlab environment with a number of realizations  $N= 1000$  for each case.

## 4 RESULTS

### 4.1 MOE random fields

The length of the weak zones are proportional to five times the dimension parallel to the axis of the pole of a single knot or group of knots. The MOE values are assigned as a function of the knot ratio ( $K$ ) of each knot or group of knots. They are correlated random variables assigned through their marginal probability function (PDF) defined for each value of  $K$ . The MOE field was calculated along each pole with the model of weak zones, explained in the section 3.1.2

As an example, Fig. 1 shows some MOE field realizations for pole 1:

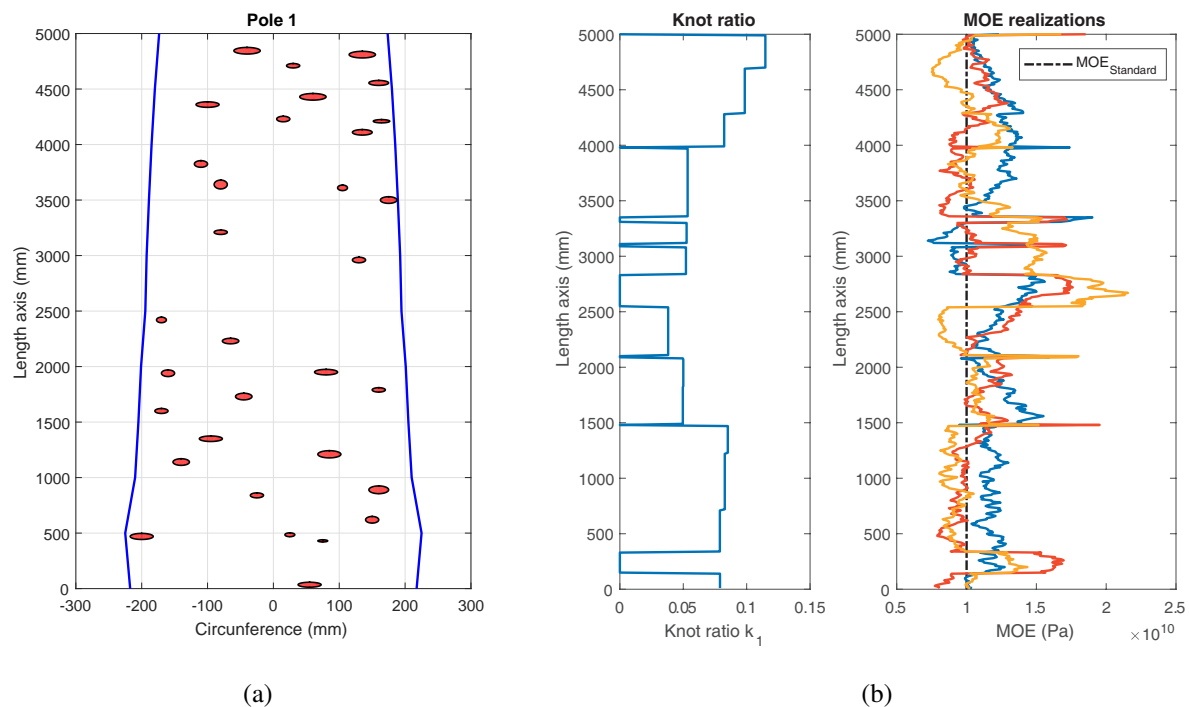


Figure 1: Weak Zone realizations. a) Record of geometry and knots from visual survey: visible knots (red dots) and circumference limits (blue lines). b) Knot ratio and MOE realizations.

Fig. 1(a) depicts the records of pole and knots geometry from visual survey for pole 1 (Gonzalez de Paz et al., 2018), when the blue lines represent the circumference limits and the red dots indicate the knots. In Fig. 1(b) the black dash dot line points out the  $MOE_{Standard}$ , which was calculated according to ASTM D 1036 (2005) standard using the load-displacement test record. It is seen that the values of the fields generated with the weak zones model and the  $MOE_{Standard}$  are similar.

### 4.2 Load-displacement results comparison

Based on the values of geometry and knots surveyed and the MOE fields, numerical models were assembled. The objective of this section was to imitate the load-displacement test. Then, the results obtained from the numerical calculations were compared with the records from the real poles. To compare the displacements, 5% and 95% percentiles were calculated on the outputs of the numerical models. The 90% of the numerical results fall within the shaded area shown in Fig. 2. The red dots represent the record test values. A tendency can also be seen

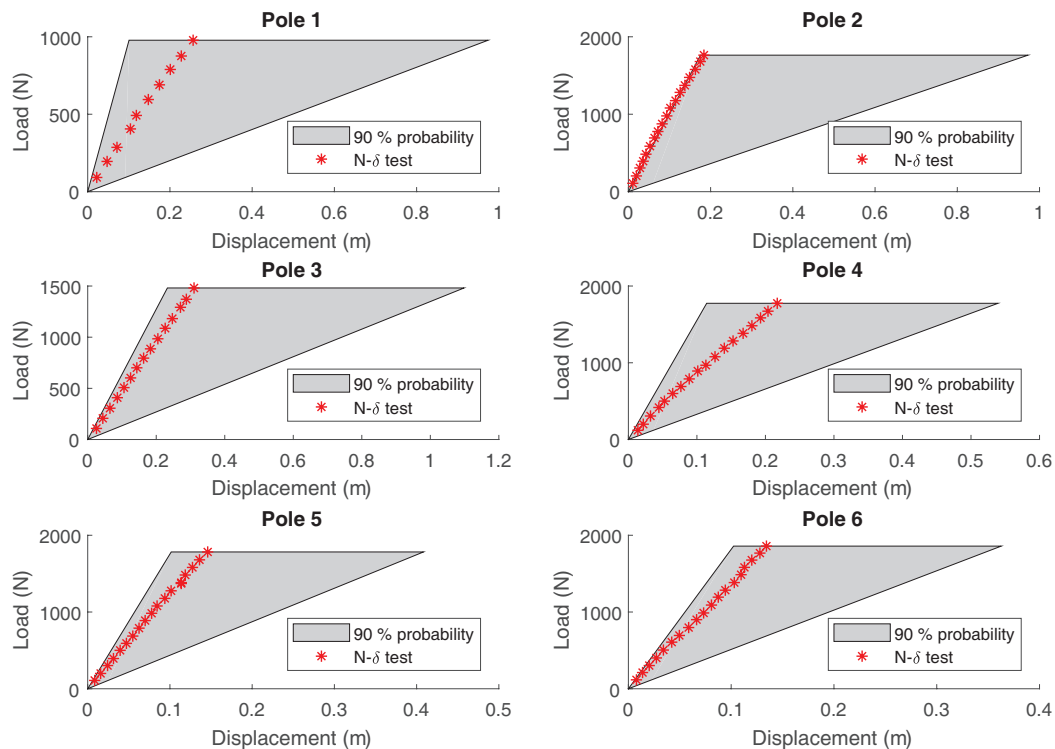


Figure 2: Numerical and Experimental load-displacement results comparison.

for the test values to be positioned in the area of the smallest displacements for a same load value. This means that the MOE fields generated by the numerical model generally result in more flexible specimens than the actual poles.

### 4.3 Natural frequencies results comparison

On the other hand, numerical models were constructed to calculate the first three natural frequencies, using the geometry surveyed, the density values determined by corresponding test and the MOE fields developed. These results were compared with the frequency values measured on the real poles.

In Fig. 3, the comparison of results from real test and numerical model is shown. The PDF for each set corresponding to each frequency was estimated and on these results, the 5% and 95% (thin lines) and 50% (dot-dash thin lines) percentiles were calculated. The frequency values obtained from tests (dot-dash thick lines) were also depicted in the graphic.

It is observed that in all cases, the three frequencies measured are between the percentiles 5% and 95%. For the first two frequencies, the experimental values are very close to the average of each distribution calculated from the simulated MOE fields. This is not the case with the third frequency.

## 5 CONCLUSIONS

The general aim of the present work was to compare the experimental approach with the numerical modeling regarding the Modulus of Elasticity (MOE) in the behavior of Eucalyptus grandis wood utility poles.

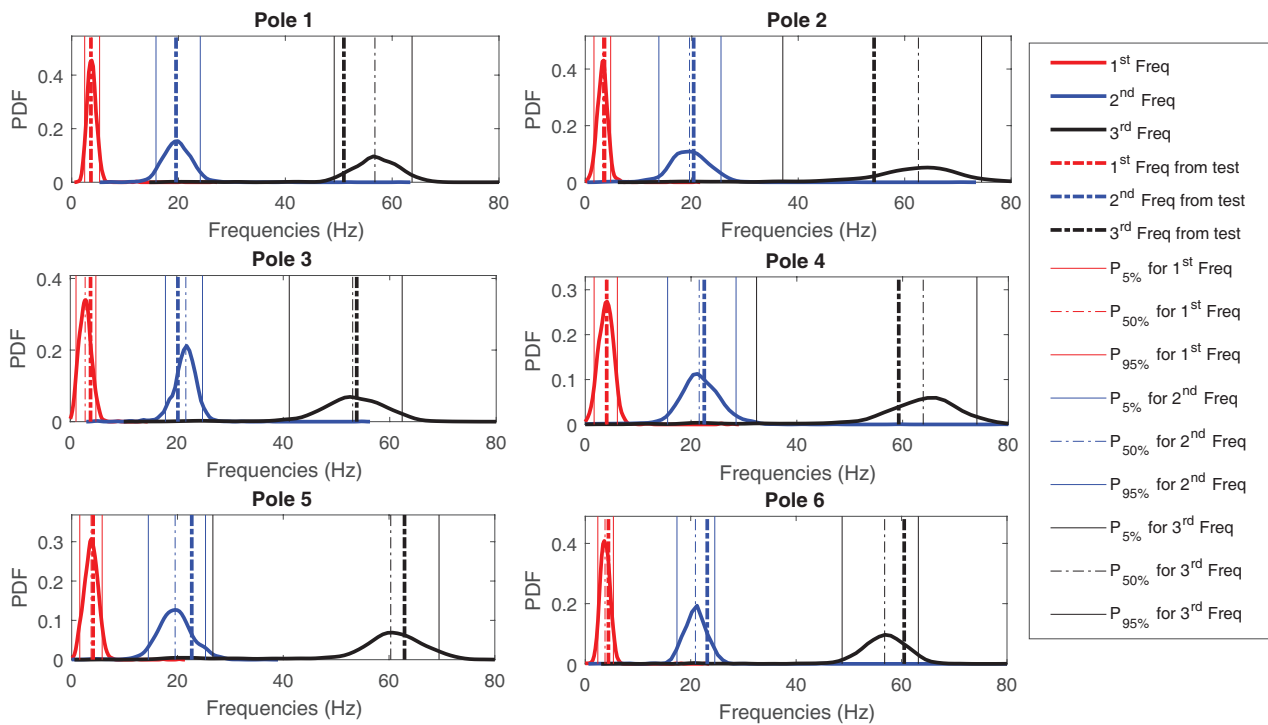


Figure 3: Numerical and Experimental frequencies results comparison.

The weak zone (WZ) model is an alternative to model the MOE taking into account the presence of knots.

The parameters  $(\mu, \sigma)$  of the MOE marginal distribution of MOE are chosen as a function of the knot ratio  $K$ . However, the parameters found in the related bibliography are valid for sawn wood. In the present study, the poles are wood structures without sawing and it not clear whether these parameters are applicable. To verify this MOE fields were calculated with the WZ model for poles whose knots were surveyed, and numerical results were compared with results of load-displacement tests and determination of natural frequencies.

It is observed that the MOE suggested by the standard lies in the range of the MOE fields obtained using the experimental data.

The results of load-displacement tests were in general within the zone of 90 % probability of occurrence, according to the simulated cases. The displacements from the test were lower than the average of the simulations for each load. The real poles, in general, result less flexible than the average of the simulations.

In the case of frequency calculation, the values recorded in the tests are within 90 % of possible values of the simulations. For the first and second frequencies, small variations were observed between the mean values of the simulations and the values registered from the tests. There were greater differences for the third frequency, which exhibits a large dispersion.

Based on these results, it can be concluded that the statistical parameters that describe the variability in the modulus of elasticity found in pieces of sawn wood of *Eucalyptus grandis*, are applicable for the simulation of wood structures without sawing, as the case of utility poles. The simulated poles are more flexible than the real poles resulting in greater displacements in the simulated cases. Therefore, using these parameters would lead to conservative results.

## ACKNOWLEDGEMENTS

The authors acknowledge the financial support of the Department of Engineering, the SGCyT-Universidad Nacional del Sur, CIC-Bs.As., ANPCyT and CONICET, all Argentinian agencies.

## REFERENCES

- ASTM D 1036. *Standard test methods of static test of wood poles*. West Conshohoken, PA, 2005.
- ASTM D 143-94. *Standard test methods for small clear specimens of timber*. West Conshohoken, PA, 2007.
- IRAM 9529. *Wood poles static flexion test methods (spanish)*. Buenos Aires, 2005.
- ANSI-05.1. *American national Standard for wood poles - Specifications and dimensions*. Washington DC, 2002.
- ASTM D 198. *Standard test methods of static test of lumber in structural sizes*. West Conshohoken, PA, 2002.
- CIRSOC 601. *Proyecto de Reglamento Argentino de Estructuras de Madera (spanish)*, 2011.
- Der Kiureghian A. and Liu P.I. Structural Reliability under Incomplete Probability Information. *Journal of Engineering Mechanics*, 112(1):85–104, 1986.
- FlexPDE, PDE. Solutions inc. <http://www.pdesolutions.com>, 2017.
- García D. Modelos numérico estocásticos de elementos estructurales de madera de eucalyptus grandis. *Universidad Nacional del Sur, Argentina*, 2017.
- García D.A. and Rosales M.B. Deflections in sawn timber beams with stochastic properties. *European Journal of Wood and Wood Products*, 75(5):683–699, 2017.
- García D.A., Sampaio R., and Rosales M.B. Vibrational problems of timber beams with knots considering uncertainties. *Journal of the Brazilian Society of Mechanical Sciences and Engineering*, pages 1–13, 2015.
- Gonzalez de Paz L.V., Garcia D.A., and Rosales M.B. Fragility curves of wood utility poles under stochastic wind load with material uncertain properties. In Martin I. Idiart and Ana E. Scarabino and Mario A. Storti, editor, *Mecánica Computacional Vol XXXIV*, pages 151–161. 2016.
- Gonzalez de Paz L.V., Garcia D.A., and Rosales M.B. Reliability of wood utility poles under stochastic wind load and material considering knots. In Martin I. Idiart and Ana E. Scarabino and Mario A. Storti, editor, *Mecánica Computacional Vol XXXV*, pages 1231–1241. 2017.
- Gonzalez de Paz L.V., Ortega N.F., and Rosales M.B. Assessment of wood utility poles deterioration through natural frequency measurements, 2018.
- ISO 3131:1975. *Wood – Determination of density for physical and mechanical tests*, 1975.
- Piter J. Clasificación por resistencia de la madera aserrada como material estructural. desarrollo de un método para el eucalyptus grandis de argentina. *Universidad Nacional de La Plata, Argentina*, 2003.
- Piter J., Zerbino R., and Blaß H. Visual strength grading of argentinean eucalyptus grandis. *Holz als Roh-und Werkstoff*, 62(1):1–8, 2004.
- Torrán E., Zitto S., Cotrina A., and Piter J.C. Bending strength and stiffness of poles of argentinean eucalyptus grandis. *Maderas. Ciencia y tecnología*, 11(1):71–84, 2009.